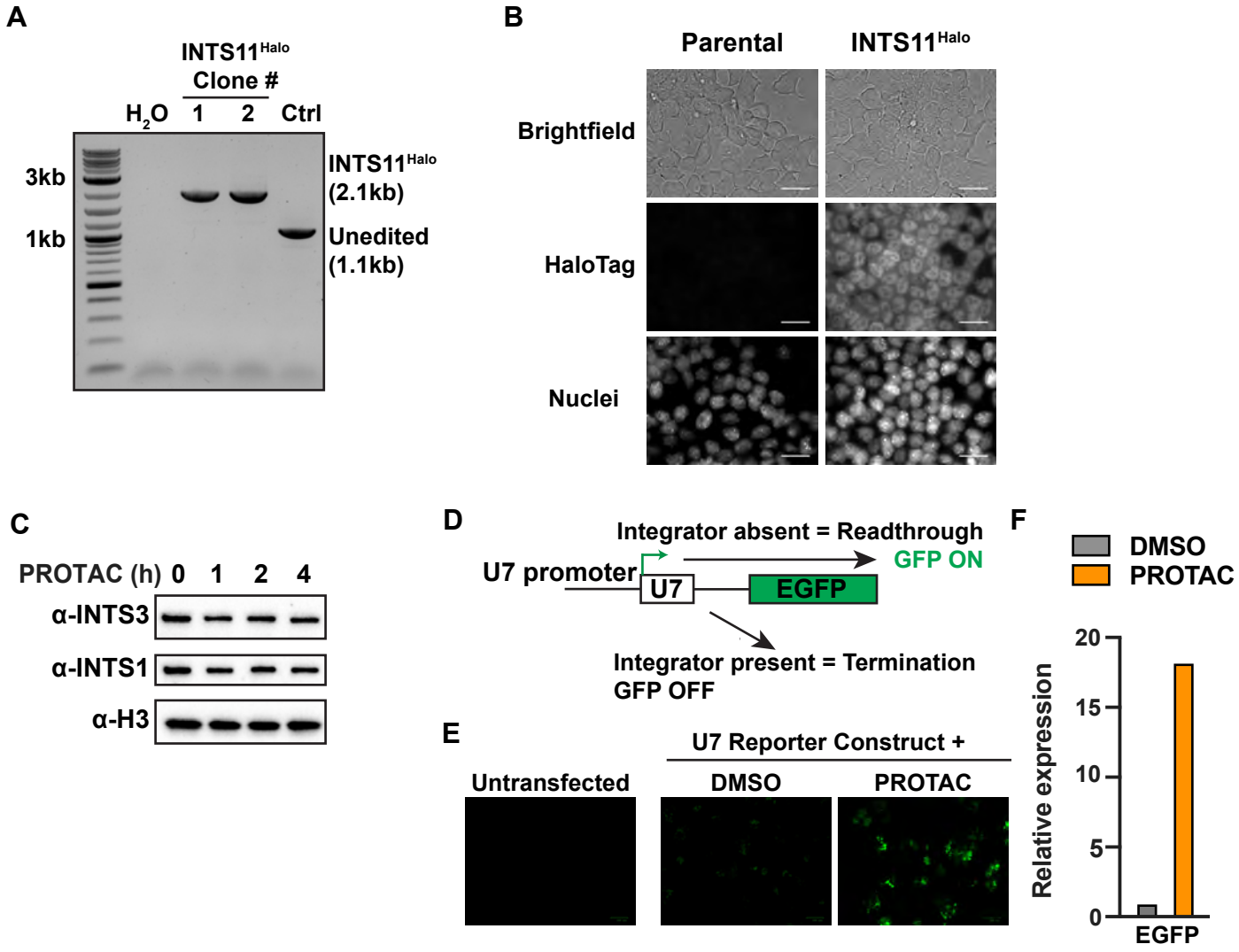

Figure S1. Related to Figure 1. Validation of INTS11^{Halo} cells

(A) PCR of genomic DNA indicating homozygous integration of the HaloTag in two clones. A negative control clone is shown to demonstrate the size of the unedited INTS11 allele.

(B) Parental and INTS11^{Halo} mESCs were differentiated to epiblast-like cells for 48 hours. Cells were stained with JFX549 to visualize the HaloTag (middle panel) and Hoechst to visualize nuclei (bottom). Scale bars represent 25 µm.

(C) Western blots of indicated Integrator subunits after PROTAC or control treatment. 0 h cells were treated with DMSO for 4h. Histone H3 was used as loading control.

(D) Schematic of reporter construct used. Green arrow indicates TSS. U7 gene body is indicated by a box. Lengths are not to scale.

(E) INTS11^{Halo} mESCs were transfected with the U7 reporter construct (except untransfected control) and 24 hours later treated with DMSO or 500 nM PROTAC for an additional 24 hours, at which point images were obtained. Scale bars represent 100 µm.

(F) Bar plot shows results of RT-qPCR from cells transfected with the U7 reporter construct. One day after transfection, cells were treated with DMSO or 500 nM PROTAC for 24 hours (n=1). Primer pair amplifies region within EGFP ORF. Value for the DMSO condition was set as 1.

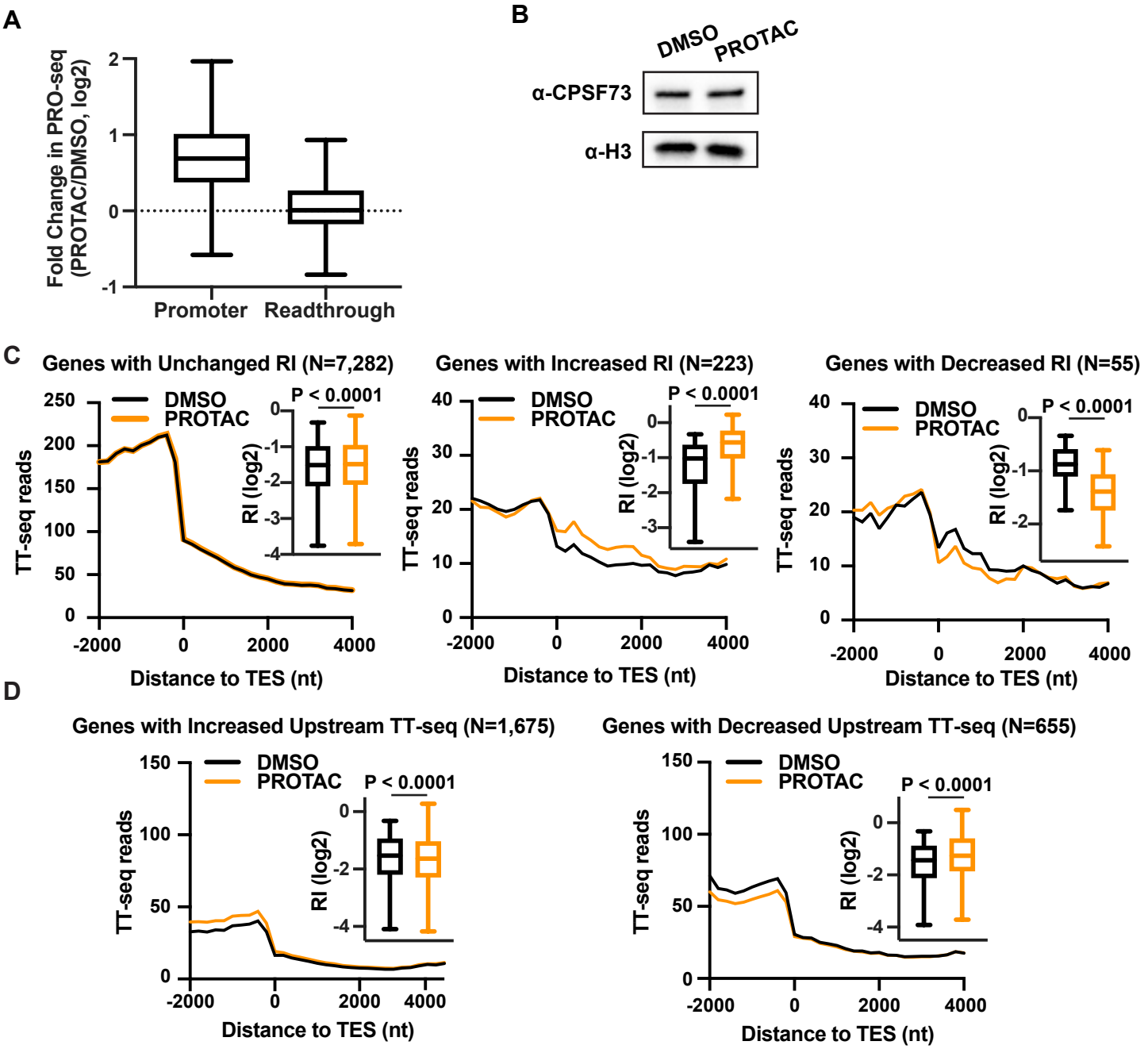

Figure S2. Related to Figure 2. Lack of evidence for INTS11 function at mRNA 3' ends.

(A) Boxplots depict fold change in PRO-seq reads near all active non-snRNA >400nt (N=16,036) promoters (TSS to +150) upon INTS11 degradation (left) and downstream of RNA 3' ends (TES to +1 kb, right). Boxes show 25th–75th percentiles and whiskers depict 1.5 times the interquartile range.

(B) Western blot of CPSF73 after 4 h DMSO or PROTAC treatment. Histone H3 was used as loading control.

(C) Metagene analysis of mRNA genes broken down by readthrough index (RI) as defined in Figure 2C. Genes with changed RI are defined as those with a difference of at least +/- 0.125 upon PROTAC treatment. Plots show average coverage of TT-seq reads in 200 nt bins. Inset boxplots depict readthrough index (RI) for the corresponding gene groups. Boxes show 25th–75th percentiles and whiskers depict 1.5 times the interquartile range. P values from Wilcoxon matched-pairs signed rank test.

(D) Metagene analysis of mRNA genes broken down by change in TT-seq reads upstream of the TES. Genes with changed TT-seq are defined as those with a difference of at $\log_2$ fold change > 0.15 in 2 kb upstream of TES . Plots show average coverage of TT-seq reads in 200 nt bins. Inset boxplots depict readthrough index (RI) for the corresponding gene groups. Boxes show 25th–75th percentiles and whiskers depict 1.5 times the interquartile range. P values from Wilcoxon matched-pairs signed rank test.

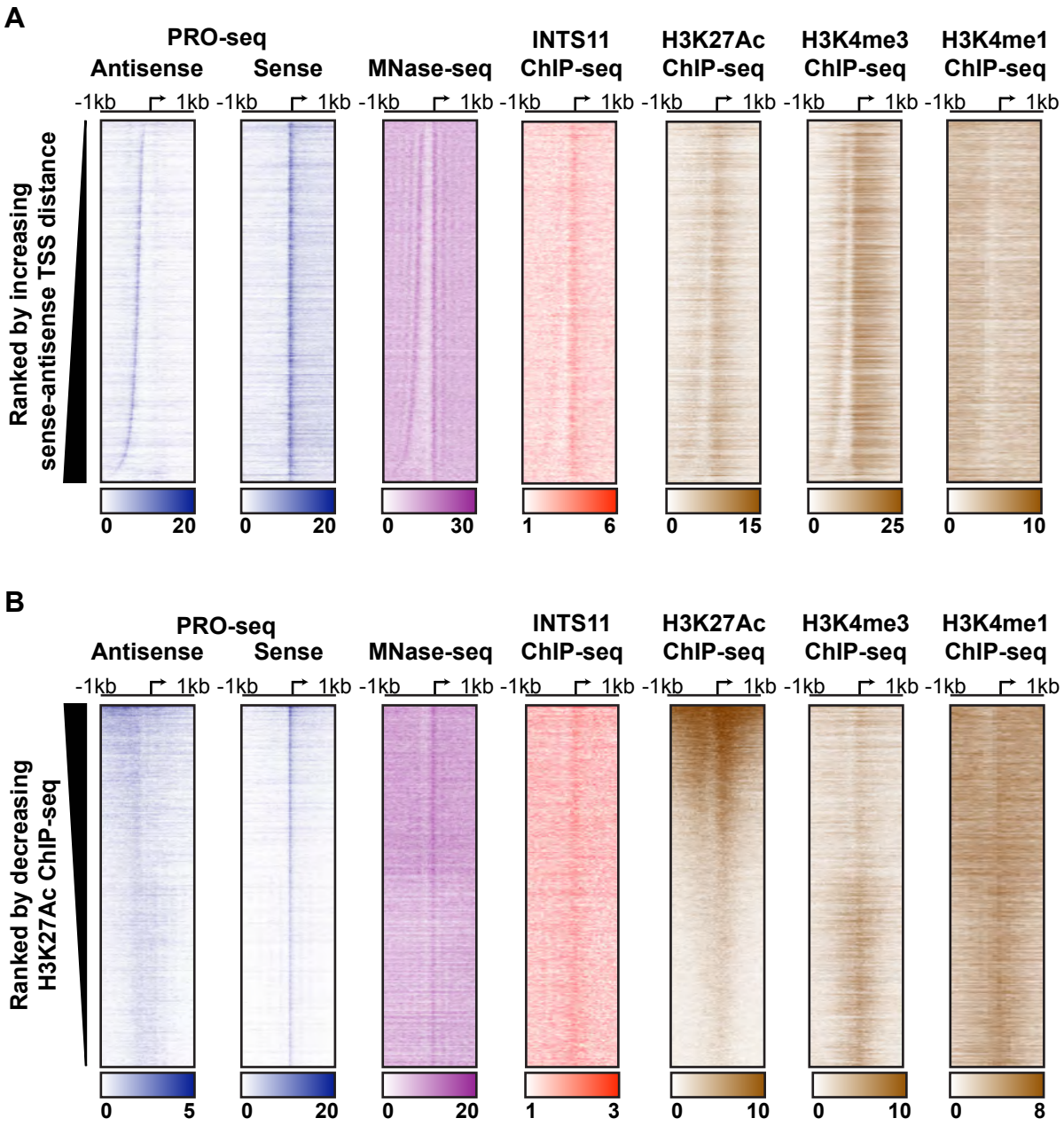

Figure S3. Related to Figure 3. uaRNAs and eRNAs show features associated with active transcription.
(A) Heatmap representation of the indicated datasets at 8,284 divergently transcribed loci ranked by increasing distance from sense TSS to antisense TSS. Arrow indicates position of sense TSS. PRO-seq and INTS11 ChIP-seq are shown from DMSO-treated cells.
(B) Heatmap representation of the indicated datasets at 9,571 intergenic sites of unannotated transcription, identified as putative enhancers, ranked by decreasing H3K27Ac ChIP-seq (TSS +/- 1 kb). Arrow indicates position of sense TSS. PRO-seq and INTS11 ChIP-seq are shown from DMSO-treated cells. Because enhancers have no inherent sense/antisense orientation, sense refers to the strongest unannotated TSS identified within the putative enhancer peak.
PRO-seq and MNase-seq are shown in 25 bp bins; INTS11, H3K27Ac, and H3K4me3 ChIP-seq are shown in 50 bp bins; H3K4me1 ChIP-seq is shown in 100 bp bins.

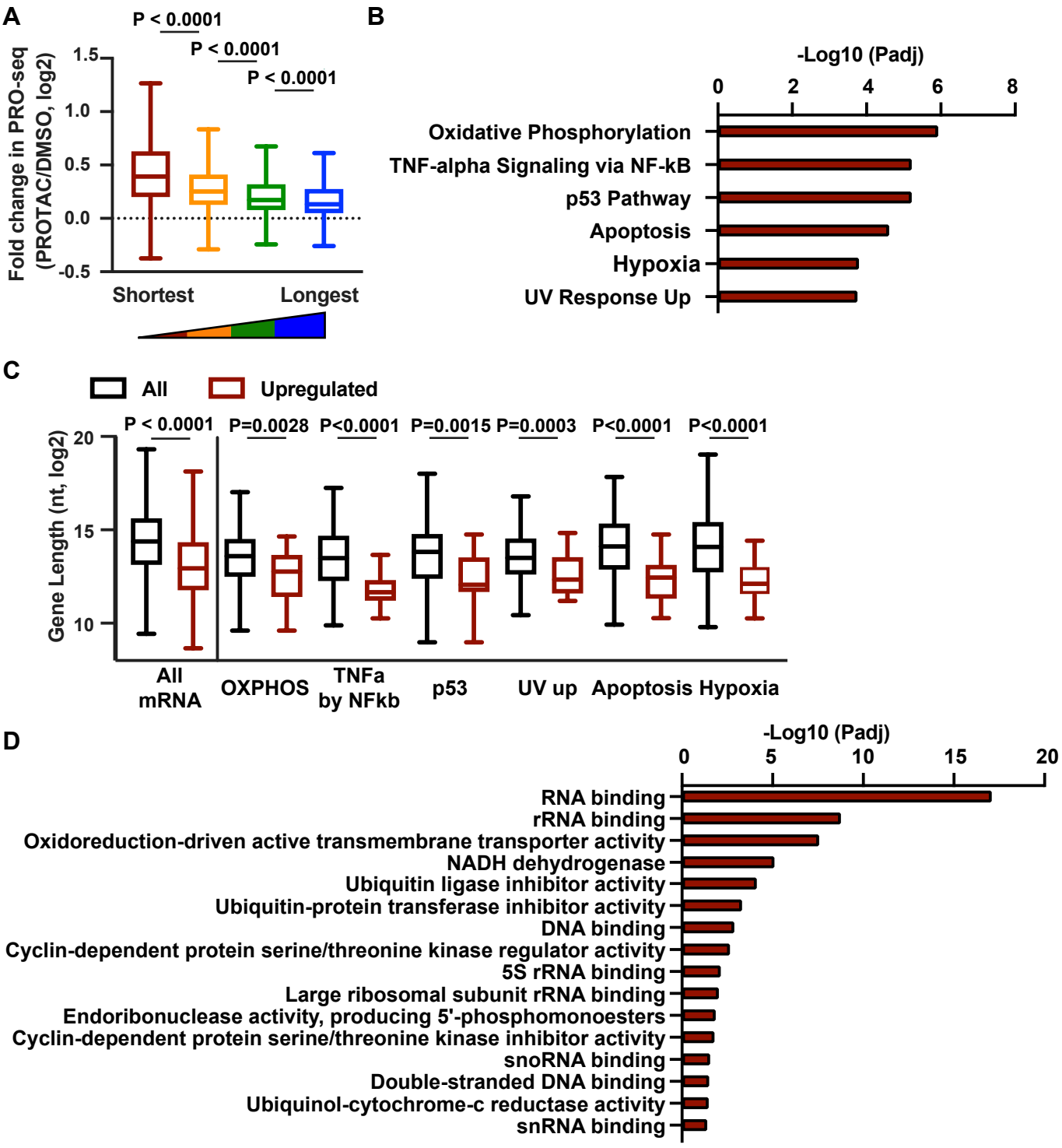

Figure S4. Related to Figure 4. Short mRNAs are most sensitive to INTS11 loss.

(A) Boxplots depict the change in whole gene (TSS to TES) PRO-seq signal after PROTAC treatment for mRNAs (N=13,057) divided into length quartiles. Boxes show 25th–75th percentiles and whiskers depict 1.5 times the interquartile range. P values from Mann-Whitney test.

(B) Gene ontology categories enriched in genes upregulated in PRO-seq (N=736) from the MSigDB Hallmark 2020 gene set. Shown are the adjusted P values for each category, for all GO terms with Padj < 0.05.

(C) The lengths of all active mRNA genes in significantly enriched GO terms as compared to those upregulated upon INTS11 depletion. Median gene lengths for each category, in nucleotides, are: All mRNAs=21,401, upregulated mRNAs=7,881, TNF-alpha=11,524, UV up=11,566, OXPHOS=12,318, p53=14,409, Hypoxia=17,394, Apoptosis=17,772. Boxes show 25th–75th percentiles and whiskers depict 1.5 times the interquartile range. P values from Mann-Whitney test.

(D) Gene ontology categories from GO Molecular Function 2021 enriched in the shortest gene quartile. Shown are categories with adjusted P values < 0.05.

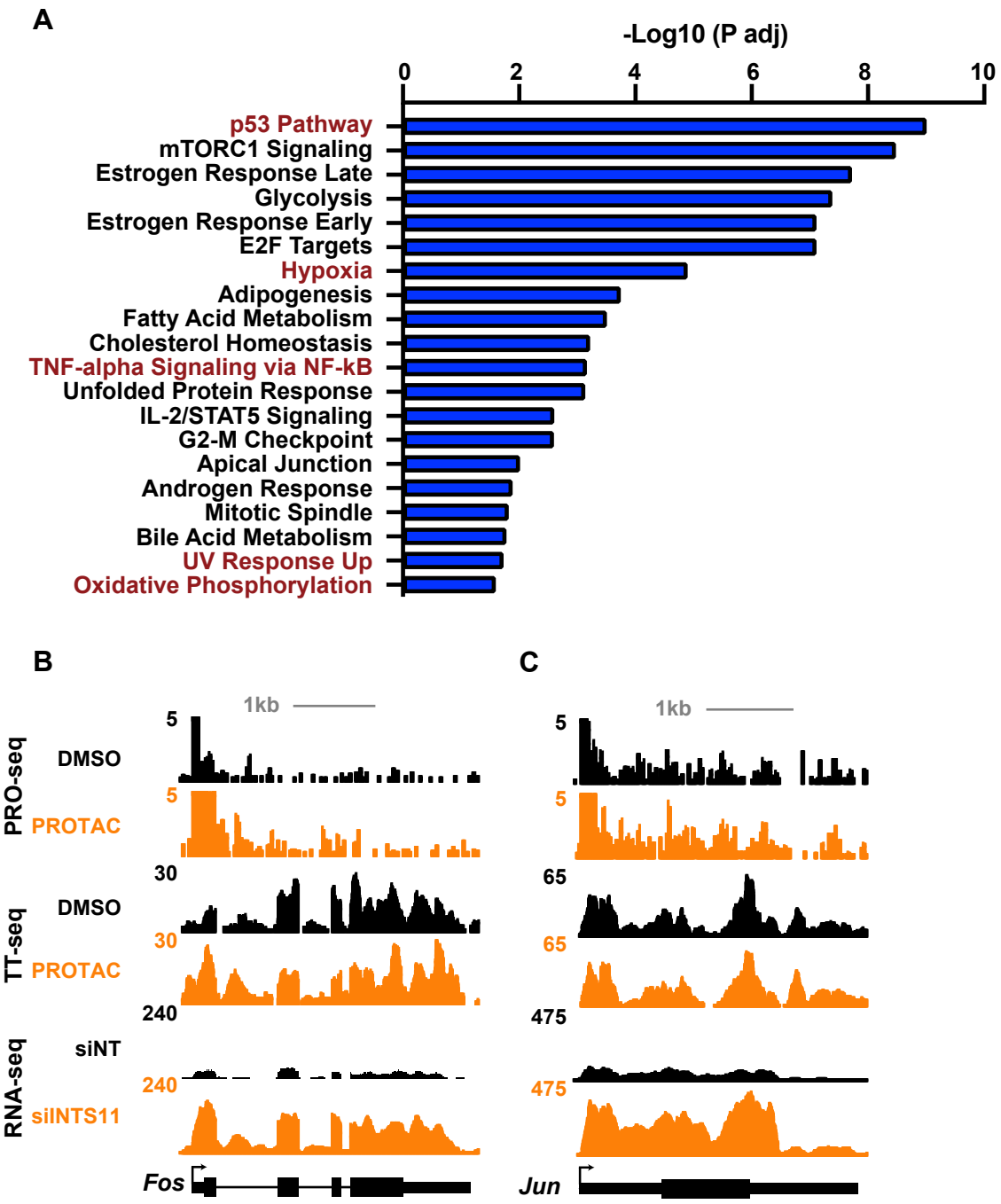

Figure S5. Related to Figure 5. Key transcription factors are upregulated following both acute and long-term INTS11 depletion.

(A) Gene Ontology (GO) analysis of the 1,681 mRNA genes downregulated upon siINTS11, as defined from RNA-seq. MSigDB terms with adjusted P value < 0.05 are shown. Terms in red were also found in GO analysis of upregulated genes from PRO-seq, as in Figure S4B.

(B-C) Example browser shots of Fos (B) and Jun (C). PRO-seq is scaled to highlight gene body signal, resulting in promoter-proximal signal extended above the window shown.

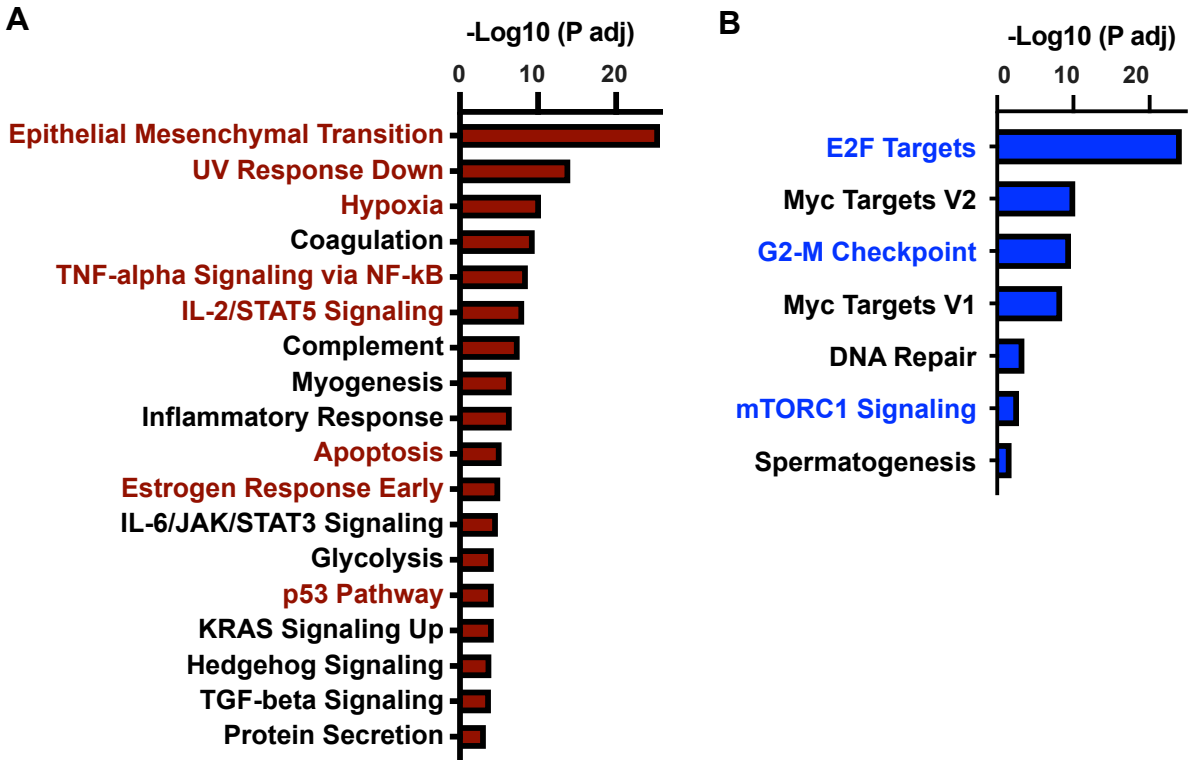

Figure S6. Related to Figure 6. Short AP-1 genes link acute INTS11 depletion to chronic INTS11 depletion.

(A) Gene Ontology (GO) analysis of the 1,000 mRNA genes upregulated upon ectopic Jun expression, as defined in Liu et al. MSigDB terms with adjusted P value < 0.05 are shown. Terms in red were also found in GO analysis of upregulated genes from siINTS11 RNA-seq, as in Figure 5E.

(B) Gene Ontology (GO) analysis of the 903 mRNA genes downregulated upon ectopic Jun expression, as defined in Liu et al. MSigDB terms with adjusted P value < 0.05 are shown. Terms in blue were also found in GO analysis of downregulated genes from siINTS11 RNA-seq, as in Figure S5A.

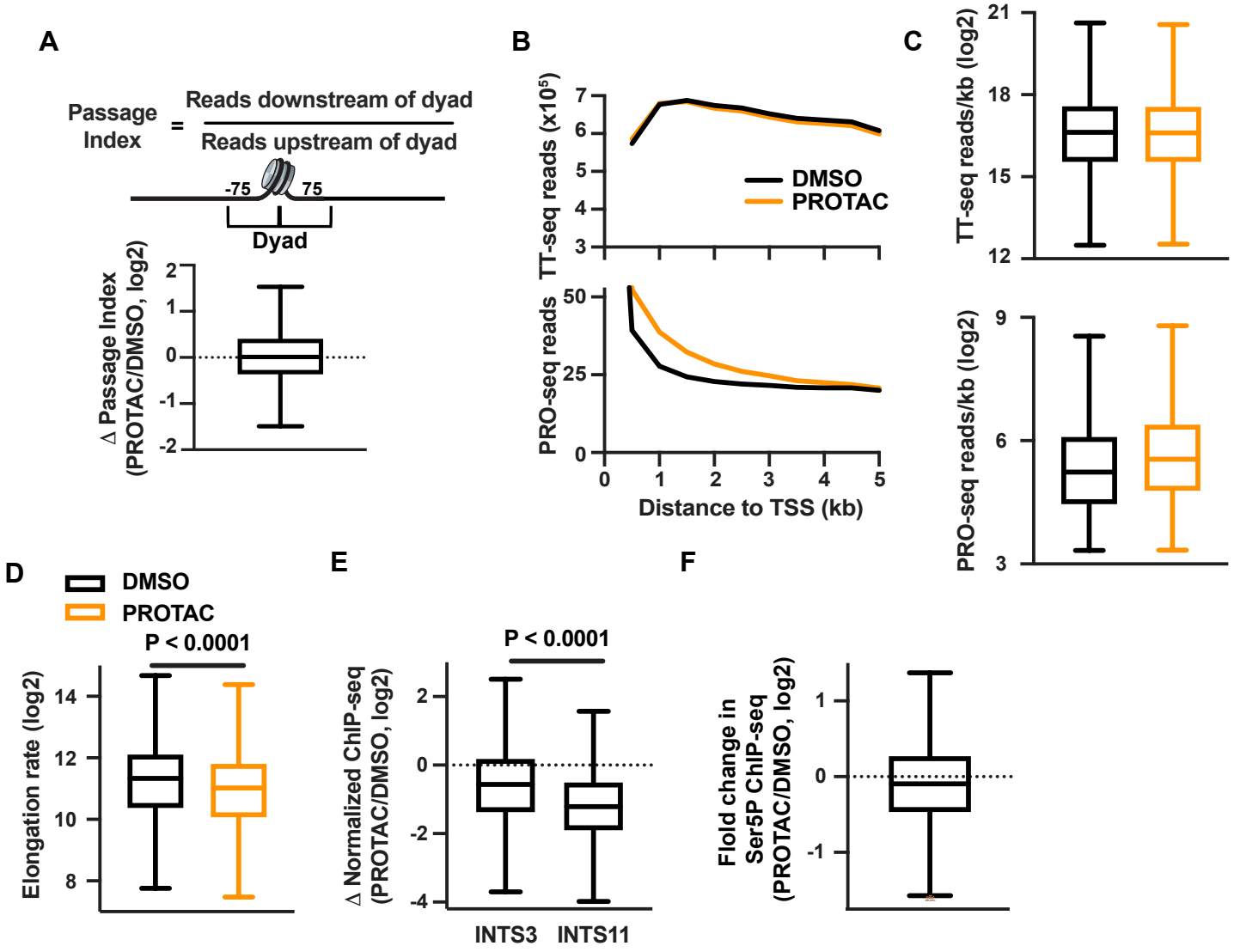

Figure S7. Related to Figure 7. The transition from early elongation to productive RNA synthesis is affected in cells lacking INTS11.

(A) Boxplot depicts the change in passage index after PROTAC treatment for mRNA genes shown in 7A and 7B. Passage Index = PRO-seq reads 75 nt downstream of dyad / PRO-seq reads 75 nt upstream of dyad. Boxes show 25th–75th percentiles and whiskers depict 1.5 times the interquartile range.

(B) Metagene analysis of TT-seq (top) and PRO-seq (bottom) signal from cells treated with DMSO or PROTAC for 4 h, aligned around TSSs of mRNA genes over 5 kb in length (N=11,247). Data are shown as average signal per gene in 500 nt bins. TT-seq signal within 500 nt of the TSS or TES was not included in this analysis, since TT-seq exhibits biased coverage at RNA 5' and 3' ends (Schwalb *et al.* 2016).

(C) Boxplots plots depict TT-seq read density (top) and PRO-seq read density (Bottom) in DMSO and PROTAC treated INTS11^{Halo} cells at mRNA genes longer than 5 kb (N=11,247). Bins were 500 nt in size, and those containing the TSS or TES were excluded. Only bins with 10 reads/kb in PRO-seq and TT-seq in both DMSO and PROTAC data were included, resulting in a total of 74,339 bins analyzed. Boxes show 25th–75th percentiles and whiskers depict 1.5 times the interquartile range.

(D) Boxplots plots depict elongation rate (arbitrary units; TT-seq read coverage/bin divided by PRO-seq reads/bin, as show in A and B). Boxplots are shown as in (A). P value from Wilcoxon matched-pairs signed rank test.

(E) Boxplots depict normalized fold change in ChIP-seq signal at active mRNA genes (N=13,055) for INTS3 and INTS11 after PROTAC treatment of INTS11^{Halo} cells. ChIP-seq signal for both Integrator subunits (TSS to +150) was normalized to PRO-seq reads (TSS to +150) to correct for the broad and substantial increase in RNAPII levels near promoters in PROTAC-treated cells. Boxes show 25th–75th percentiles and whiskers depict 1.5 times the interquartile range. P value is from Wilcoxon matched-pairs signed rank test.

(F) Boxplot depicts fold change in ChIP-seq signal at active mRNA genes (N=13,055) for Ser5P after PROTAC treatment of INTS11^{Halo} cells. Boxes show 25th–75th percentiles and whiskers depict 1.5 times the interquartile range.

Supplementary Tables

Table S1. Genes encoding Transcription Factors are upregulated by acute INTS11 depletion. Related to Figure 4. List of transcription factors identified as significantly upregulated in PRO-seq experiments performed on DMSO- and PROTAC-treated $INTS11^{Halo}$ cells (N=48). The threshold to define differentially expressed genes was fold change > 1.5 and adjusted P value < 0.01. Fold change (log2) is shown for each gene, along with gene name and symbol.

Table S2. Oligonucleotide sequences used in this study. Related to STAR Methods.

Table S1. Genes encoding Transcription Factors are upregulated by acute INTS11 depletion. Related to Figure 4.

Ensembl Gene ID	Gene Name	Fold Change in PRO-seq (log2)
ENSMUSG00000007872	ID3	0.730
ENSMUSG00000014030	PAX5	0.995
ENSMUSG00000020644	ID2	1.423
ENSMUSG00000021250	FOS	1.347
ENSMUSG00000021359	TFAP2A	0.888
ENSMUSG00000021379	ID4	0.854
ENSMUSG00000022346	MYC	0.628
ENSMUSG00000022528	HES1	0.723
ENSMUSG00000022952	RUNX1	0.837
ENSMUSG00000023882	ZFP54	1.098
ENSMUSG00000023892	ZFP51	0.676
ENSMUSG00000024420	ZFP521	0.585
ENSMUSG00000025408	DDIT3	0.644
ENSMUSG00000025592	DACH2	0.588
ENSMUSG00000026628	ATF3	0.655
ENSMUSG00000027230	CREB3L1	0.703
ENSMUSG00000029127	ZBTB49	0.664
ENSMUSG00000029135	FOSL2	0.832
ENSMUSG00000029627	ZKSCAN14	0.887
ENSMUSG00000032446	EOMES	0.639
ENSMUSG00000034429	ZFP707	0.817
ENSMUSG00000034486	GBX2	0.831
ENSMUSG00000034957	CEBPA	0.890
ENSMUSG00000037447	ARID5A	0.669
ENSMUSG00000041540	SOX5	0.728
ENSMUSG00000042745	ID1	1.151
ENSMUSG00000042821	SNAI1	0.924
ENSMUSG00000044636	CSRNP2	0.867
ENSMUSG00000044646	ZBTB7C	0.693
ENSMUSG00000050619	ZSCAN29	0.739
ENSMUSG00000051341	ZFP52	0.634
ENSMUSG00000052684	JUN	0.948
ENSMUSG00000054381	ZFP747	0.777
ENSMUSG00000056383	AI987944	0.601
ENSMUSG00000057098	EBF1	0.850
ENSMUSG00000057409	ZFP53	0.657
ENSMUSG00000057835	ZFP119A	0.589
ENSMUSG00000063568	JAZF1	0.682
ENSMUSG00000067071	HES6	0.925
ENSMUSG00000071302	2610044O15RIK8	0.624
ENSMUSG00000071637	CEBPD	0.910
ENSMUSG00000074166	AW146154	0.681
ENSMUSG00000074472	ZFP872	1.056
ENSMUSG00000074862	BC025920	0.789
ENSMUSG00000075327	ZBTB2	0.605
ENSMUSG00000078872	GM14401	0.693
ENSMUSG00000079033	MEF2B	0.611
ENSMUSG00000109398	GM3854	0.675

Table S2. Oligonucleotide Sequences

RT-qPCR Primers	Forward Primer	Reverse Primer
U1	TAGGCACAGTCGTGTCTTACTA	GAAACCCGCAACTCCTTACA
U2	ATCTCACGTAGGACCTCTTATTTC	CTCACCTTGTTCCTGACTGTAT
EGFP	CTGGACGGCGACGTAAAC	CGGTGGTGCAGATGAACTT
TBP	GAAGAACAATCCAGACTAGCAGCA	CCTTATAGGGAACTTCACATCACAG

CRISPR lines	sgRNA Oligo F	sgRNA Oligo R
HaloINTS11	CACCCAAGGGAGTGACCCTAATCT	AAACAGATTAGGGTCACTCCCTTG

PCR primers	Forward Primer	Reverse Primer	Notes
CAST Homology Arm Left	TGTAATACGACTCACTATAGGGCGAATTCGAGCTGCATCCCTCTGATGATCAAGCTAAAC	AACAGCCGCCAGCCGCTCACCATGGTCAGGGAGGTCGC	For making left homology arm of CAST CRISPR repair construct
CAST Homology Arm Right	TGTACTTTCAGAGCGATAACATGCCtGAGATTAGGGTCAC	GAGCGCAGCGAGTCAGTGAGCGAGGAAGCTCTTCTacaattcgggatagaccagacacaa	For making right homology arm of CAST CRISPR repair construct
129 Homology Arm Left	TGTAATACGACTCACTATAGGGCGAATTCGAGCTGCATCCCTCTGATGATCAAGCTAAAC	AACAGCCGCCAGCCGCTCACCATGGTCAGGGAGGTCGC	For making left homology arm of 129 CRISPR repair construct
129 Homology Arm Right	TGTACTTTCAGAGCGATAACATGCCtGAGATTAGGGTCAC	GAGCGCAGCGAGTCAGTGAGCGAGGAAGCTCTTCTacaattcgggatagaccagacacaa	For making right homology arm of 129 CRISPR repair construct
INTS11_genomic	TGGGCTCACCTTGTGTTTAG	gcactggctctgaaactgtctactc	For screening and sequencing CRISPR clones